Electron-Promoted Desorption from Water Ice Surfaces: Neutral Gas-Phase Products

Ali G. M. Abdulgalil, Alexander Rosu-Finsen,[*] Demian Marchione,[†] John D. Thrower,[‡] Mark P. Collings and Martin R. S. McCoustra[*]

Institute of Chemical Sciences, Heriot-Watt University, Riccarton, EH14 4AS, Edinburgh, United Kingdom.

ABSTRACT

Electron-promoted desorption (EPD) from compact amorphous solid water (c-ASW) has been studied. Low-energy electron bombardment with 200 to 300 eV electrons leads to H_2O depletion as monitored by reflection-absorption infrared spectroscopy (RAIRS) of the remaining c-ASW film. Cross-sections for H_2O depletion were calculated to be in the range $1.6\pm1.0 \times 10^{-16}$ to $5.2\pm3.0 \times 10^{-16}$ cm^2. However, mass spectrometric measurements identify a major component of the desorbing material as H_2, which appears with similar kinetics to those for H_2O loss. Molecular H_2O is observed as a minor desorption product in the gas phase.

1. Introduction

Water (H_2O), in its solid and gaseous forms, is a key molecule in the Solar System and beyond. It has been detected in both forms in many galactic environments including planets, comets, and the interstellar medium (ISM) itself.[1] Observations show that H_2O is a major component of interstellar ices along most lines-of-sight, with a typical abundance of 1×10^{-4} with respect to atomic hydrogen.[2] The formation of H_2O ice in astrophysical environments occurs at low pressure and low temperatures (10-90 K). The dominant H_2O formation pathway in the ISM is through reactive accretion involving efficient atomic oxygen (O),[3] molecular oxygen (O_2),[4,5] and ozone (O_3)[6] hydrogenation directly on grain surfaces. Gas-phase H_2O formation followed by freeze-out onto grain surfaces does not account for observed solid H_2O abundances.[7] In most astrophysical environments, H_2O is found to exist as amorphous solid water (ASW) which is metastable with respect to the crystalline state due to a high activation barrier for the structural transformation.[8,9]

During the formation of dense cores, freeze-out of gas phase species onto the surfaces of dust grains takes place, adding to the icy mantles created by reactive accretion. At the low temperatures (<20 K) found in dense regions, these ices will adsorb a variety of chemical species.[10,11] As the core density increases and a protostar is formed and begins to heat its environment, thermal desorption begins to return the species locked in the ices to the gas phase.[12-17] Non-thermal processes, however, can liberate species under conditions where they cannot be thermally evaporated. The key non-thermal process is assumed to be photodesorption driven by VUV photons.[18,19] However, cosmic rays,[20] electrons[21,22] and longer wavelength optical[23] radiation can also promote desorption.

Laboratory experiments focusing on the thermal desorption of H_2O have enhanced our knowledge of H_2O-based ices on model interstellar dust grains.[24-26] These experiments have revealed how H_2O binds with different surfaces and show that H_2O islands are formed on surfaces such as SiO_2 due to the dominance of H_2O-H_2O interactions over those of H_2O-SiO_2. *i.e.* H_2O de-wets from the silica surface. Furthermore, infrared spectroscopic experiments have shown that H_2O begins to de-wet from the SiO_2 surface at temperatures below 40 K.[26,27]

Electron-promoted desorption (EPD) is of interest to the astrophysical community due to the wide array of energetic ionizing radiation interacting with interstellar ice surfaces. As radiation passes through the molecular ice film such interactions result in an abundance of secondary electrons and secondary electronic excitations. A variety of EPD experiments have been performed, both with H_2O itself and with molecules adsorbed on a H_2O film. Such experiments have, for instance, shown D^+ formation from pure D_2O when bombarding the film with a 100 eV electron beam;[28] H_2, O_2 and H_2O_2 formation in a pure H_2O film after irradiation with 5 keV electrons;[29] and morphological changes have also been observed.[30,31] More recent studies have highlighted an efficient non-thermal desorption mechanism for species weakly hydrogen-bonded to the ASW surface mediated by the transport of excitons with energies of 8-12 eV.[21,32] However, there is a perception that radiation-driven non-thermal desorption is akin to thermal desorption and hence can be used to explain the observation of molecular species in cold, dense environments *e.g.* H_2O,[33] methanol[34] and acetonitrile.[35] The majority of experiments in the astrochemical literature, however, look at surface loss as a guide to desorption rate and do not look to the nature of the species leaving the surface, which may be dominated by fragments and reaction products rather than the parent ice species. An interesting conclusion then follows that EPD of COMs may therefore not lead to intact COMs in the gas-phase, but rather their molecular

fragments. Literature data, however, shows that simple species, *e.g.* C_6H_6, weakly hydrogen-bonded to the surface of water films may desorb efficiently as intact molecules. The observations reported herein, however, suggest that we must be cautious with extrapolating that observation to molecules buried in the near-surface bulk. This work opens a window on that question by reporting the detection of molecular hydrogen (H_2) during EPD of ASW and a comparison of the kinetics of its appearance with our previously reported H_2O loss data.

2. Experimental Method

The ultrahigh vacuum (UHV) chamber, with a base pressure of lower than 2×10^{-10} mbar, and ancillary experimental equipment have been described in detail previously.[36] A brief description of the experimental procedure is provided herein. The substrate was a polished stainless steel disc coated with a 200 nm film of amorphous silica ($aSiO_2$) deposited by electron beam evaporation as described previously.[36] The substrate was cooled through contact with a liquid nitrogen reservoir, reaching a base temperature of 112 K as measured by a K-type thermocouple spot-welded to the edge of the stainless steel disc. Molecules were background dosed onto the $aSiO_2$ film in units of Langmuir (L, where 1 L represents an exposure of 1.0×10^{-6} Torr for 1 s). Film thickness, *d,* can then be estimated from Equation 1:

$$d = \frac{SPt}{\sqrt{2\pi m k_B T}} \times \frac{1}{\rho_S} = \frac{Z_W t}{\rho_S} \qquad (1)$$

where S is the sticking coefficient assumed to be unity, P is the pressure recorded with the ion gauge with the approximate molecular ionization efficiency of 1.1 for H_2O,[37] t is the exposure time, k_B is the Boltzmann constant, T is the temperature of the dosed molecules, Z_W is the bombardment rate (the incident flux), ρ_S is the molecular volume density and m is the molecular

mass. Electron irradiation of H_2O films was done with an ELG-2 (Kimball Physics) electron gun with energies as stated in the following paragraphs.

In our original experiments,[38] a 20 L ASW film was deposited corresponding to an estimated average film thickness of 2.4±0.2 nm. However, in the light of our knowledge of such films, the H_2O is likely present on the silica surface in the form of islands several molecules thick.[27] Electron irradiation was performed with an angle of 45° with respect to the surface normal and with electrons having energies in the range of 200-300 eV with an energy spread of 0.5 eV. The electron beam was rastered over the approximately 0.75 cm^2 of substrate surface with a frequency of 2 s^{-1} and this resulted in a typical electron flux of up to $(1.7±0.1) \times 10^{12}$ electron cm^{-2} s^{-1}. Changes in the ASW film during electron irradiation were monitored using reflection-absorption infrared spectroscopy (RAIRS) at a grazing angle of 86° to the substrate normal. RAIR spectra were acquired by the co-addition of 1024 scans with a resolution of 2 cm^{-1} as collected by a liquid N_2 cooled MCT detector using a BioRad Model FTS-80 FT-IR spectrometer. The data we use from reference 38 can be seen in Figure 1 (ii) and is discussed in the following text.

In the more recent experiments, thicker ASW films, typically exposures of 150 L and hence thickness of around 18±2 nm, were investigated. Both H_2O and D_2O were investigated and each film had 1 L of benzene (C_6H_6) deposited on top of the ASW films. The presence of the C_6H_6 reflecting the original intent of the work to probe exciton-mediated desorption.[21,32,38] The data and results presented in this work come as a fortuitous addition to that story in the light of a more thorough review of our data. At this exposure, C_6H_6 is present as small islands dispersed over the H_2O/D_2O surface with isolated molecules diffusing between.[32] As such the H_2O solid surface itself is largely unobscured. Thus, the islanded C_6H_6 overlayer does not significantly impact on

desorption of the ASW substrate. Electron irradiation was performed at *ca.* 30° with respect to the substrate normal giving an irradiated area of 1 mm^2. CASINO simulations indicate that the electrons penetrate deeply into the ASW.[21] The electron beam was not rastered in these measurements. The resulting average electron flux was $(9.0\pm2.0) \times 10^{13}$ electron cm^{-2} s^{-1}, typically with a value of $(1.1\pm0.2) \times 10^{14}$ electron cm^{-2} s^{-1} in the first 50 s and quickly reaching a limiting value of $(7.5\pm0.5) \times 10^{13}$ electron cm^{-2} s^{-1} at longer times. Substrate charging is believed to be the reason for the change in electron flux as reported previously in studies of electron irradiation of thin films in the same UHV chamber.[21] The evolution of gas phase H_2 and other species (m/z = 2, 16 and 18) from the electron irradiated ASW film was monitored by a cross-beam source, quadrupole mass spectrometer (VG Microtech PC300D, further modified by European Spectrometry Systems) with a homemade line-of-sight tube facing the front of the substrate upon which the molecular film is deposited.

3. Results and Discussion

We begin by summarizing our previously reported observations.[38] RAIR spectra in the region of the ν_{OH} stretching bands following electron irradiation of 14 L of H_2O adsorbed on the $aSiO_2$ surface show a clear and significant decrease in intensity of the ν_{OH} stretching band with increasing time of exposure to the electron beam as the ASW film is irradiated. No other changes in the entire IR spectrum are observed during irradiation suggesting that no significant concentration of new chemical species are being formed and then retained in the ice on the timescale of our experiment. Figure 1 shows the behavior of the integrated intensity of the ν_{OH} stretching band with exposure time for a number of incident electron energies. The total EPD

cross-section, σ_{EPD}, is derived from the first-order loss of H_2O from the ASW film assuming we are in the thin film limit:[39-41]

$$-\frac{dC}{dt} = k_{EPD}C = \varphi\,\sigma_{EPD}\,C \qquad (2)$$

where C is the surface concentration of H_2O in cm^{-2}, k_{EPD} is the rate constant for EPD and φ is electron flux in electrons $cm^{-2}\ s^{-1}$. By integrating Equation 2, we can describe the exponential decays in Figure 1 in terms of their decay time constant or life-time, τ.
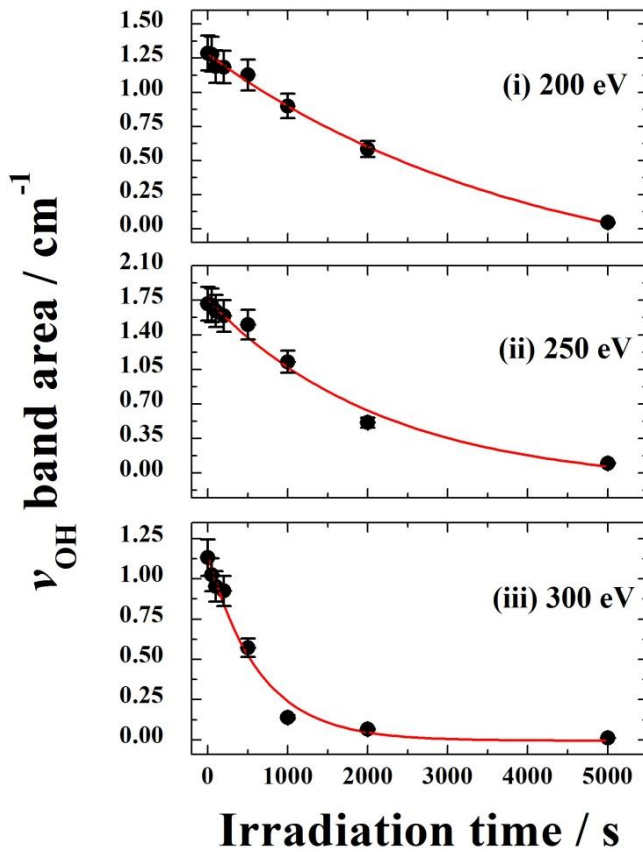
Figure 1. Decay of the integrated ν_{OH} stretching band intensity as a function of irradiation time (black symbols) along with the fitted exponential decay function (red line). Electron energies are: (i) 200 eV, (ii) 250 eV, and (iii) 300 eV. The thickness of the 150 L H_2O film is 18 nm and 0.035 nm for the 1 L C_6H_6 film present as islands on the H_2O film.

Electron energy / eV	Electron flux / electron cm^{-2} s^{-1}	EPD cross section / cm^2
200	$(1.4\pm0.1) \times 10^{12}$	$(1.6\pm0.1) \times 10^{-16}$
250	$(1.7\pm0.1) \times 10^{12}$	$(3.2\pm0.4) \times 10^{-16}$
300	$(1.6\pm0.1) \times 10^{12}$	$(5.2\pm0.6) \times 10^{-16}$

Table 1: The calculated total cross-section of H_2O loss, EPD cross-section, observed through RAIRS. The error on the electron flux is due to the ammeter accuracy while the cross sections have uncertainties due to the ammeter accuracy as well as the exponential decay functions of Figure 1.

The total cross-section for H_2O loss, σ_{EPD}, is then calculated from Equation 3:

$$k_{EPD} = \frac{1}{\tau} = \varphi\,\sigma_{EPD} \qquad (3)$$

where the incident electron flux was scaled to take into account the 2 s^{-1} raster. Table 1 summarizes the calculated cross-sections for H_2O loss. These results indicate that the cross-section increases monotonically with increasing electron energy. The results seem to suggest that the cross-section increases monotonically with increasing electron energy. This can be explained in terms of a combined effect of a greater penetration depth, and larger yield of secondary electrons and excitations, when irradiating the ice with more energetic electrons. However, more experiments are needed in order to confirm this hypothesis.

It is worth re-iterating at this point that the cross-sections in Table 1 are many orders of magnitude larger than the reported cross-sections for photon-stimulated desorption in the VUV, which are typically of the order of ~10^{-18} cm^2 and ~10^{-19} cm^2 in the near UV-Visible for doped ASW.[38,42] This would imply that electron-promoted desorption, initiated by cosmic ray

interactions in icy grains, could be the primary non-thermal desorption mechanism in cold, dense regions in the ISM.[38]
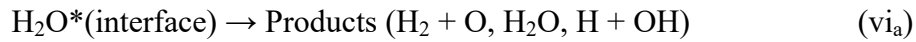
Figure 2 shows desorption signals as a function of irradiation time for the electron irradiation of 1 L of C_6H_6 on solid H_2O (left panel) and on solid D_2O (right panel). The recorded traces for m/z = 2 (H_2), = 4 (D_2), and = 16 (O) are fully consistent with H_2[43] and O_2[44,45] forming during the electron irradiation of thick pure ASW. The m/z = 16 signal can be attributed to both O atoms and O_2 which is seen to increase and reach a plateau.
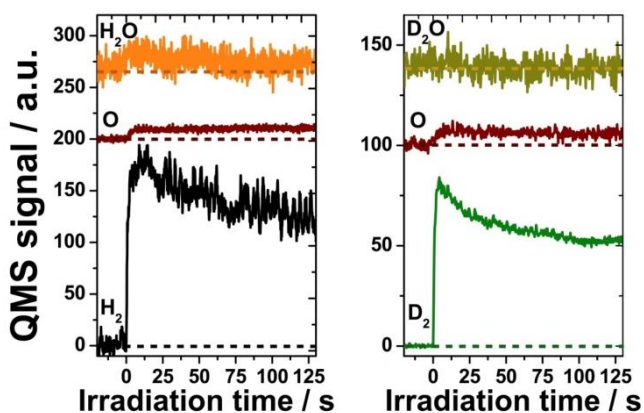
Figure 2. Time dependence of the QMS signals in m/z channels 2 [4] (H_2 [D_2]), 16 (O) and 18 [20] (H_2O [D_2O]) during irradiation of 1 L of C_6H_6 on a thick ice of solid H_2O (150 L) and on solid D_2O (150 L) in the left and right panels, respectively. Irradiation starts at t=0 s with 250 eV electrons. Traces have been offset for clarity with the dashed lines showing the zero lines for each curve.
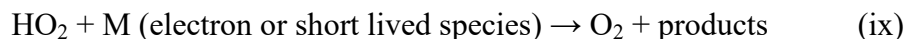
Kimmel and co-workers have thoroughly investigated the chemistry occurring in H_2O ices deposited on Pt(111) upon irradiation with low energy electrons (*e.g.* 100 eV, 87 eV). They first observed molecular hydrogen formation in earlier work[43] and discussed the mechanism of such electron induced chemistry (EIC) in subsequent work.[46,47] The data in Figure 2 is consistent with

the so-called *prompt* desorption of H_2 that forms at the ASW interface as reported in the previously mentioned literature, despite the presence of 1 L of C_6H_6 as an adlayer. The evident agreement of our data with these earlier findings suggests that dehydrogenation of the aromatic molecule mediated by the H_2O substrate is not significant and can be considered as negligible, at least for C_6H_6/ASW. It follows that some of the reactive steps involved in the observed H_2 production are:[46]

$$H_2O + e^- \rightarrow H_2O^+ + 2e^-_{NT} \tag{i}$$

$$H_2O^+ + H_2O \rightarrow H_3O^+ + OH \tag{ii}$$

$$e^-_{NT} \rightarrow e^-_{TE} \tag{iii}$$

$$H_2O^+ + e^-_{TE} \rightarrow H_2O^*(bulk) \tag{iv$_a$}$$

$$H_3O^+ + e^-_{TE} \rightarrow H_3O^*(bulk) \tag{iv$_b$}$$

$$H_2O^*(bulk) \rightarrow H_2O^*(interface) \tag{v$_a$}$$

$$H_3O^*(bulk) \rightarrow H_3O^*(interface) \tag{v$_b$}$$

$$H_2O^*(interface) \rightarrow Products\ (H_2 + O, H_2O, H + OH) \tag{vi$_a$}$$

$$H_3O^*(interface) \rightarrow Products \tag{vi$_b$}$$

This mechanism initially involves direct excitation of H_2O molecules leading to secondary electrons and ions. Then a sequence of inelastic scattering events thermalize the non-thermal primary electrons (e^-_{NT}) inside the bulk, leading to electronic excitations and trapped thermal electrons (e^-_{TE}) culminating with electron-ion recombination. Excitons (electronically excited molecules generated by absorption of a quantum of energy corresponding to a molecular orbital

transition) are produced along the track of the incident electron beam in the solid. Such excitons can be localised on a single molecule or are free to move throughout a solid. In solid H_2O, there is much experimental evidence that the excitons are mobile and able to diffuse from their point of generation to the surface probably via a non-radiative resonant energy transfer mechanism.[21,32,48] Molecular oxygen (O_2) formation has also been observed and investigated by Petrik *et al.*[44,45] and requires additional steps to those listed above involving the accumulation of precursors, such as H_2O_2 and HO_2, in order to release O_2 starting from the OH produced at the vacuum interface by the reactions (vi_a) and (vi_b):

$$2OH \rightleftharpoons H_2O_2 \qquad\qquad\qquad\qquad\qquad\qquad\text{(vii)}$$

$$OH + H_2O_2 \rightarrow HO_2 + H_2O \qquad\qquad\qquad\qquad\text{(viii)}$$

$$HO_2 + M \text{ (electron or short lived species)} \rightarrow O_2 + \text{products} \qquad\text{(ix)}$$

where M is an unknown reaction partner that can be either an energetic electron or a short-lived species. By comparing the EIC curves corresponding to H_2 and D_2, one might note that the former is almost twice as intense as the latter. This can be explained simply as different sensitivities for the ion signal corresponding to m/z = 2 and = 4 of the QMS. However, this observation may also infer an actual effect of isotopic substitution. Further studies are required to clarify this observation. It could simply be a classical kinetic isotope effect due to changes in the zero-point and transition state vibrational energies of the two isotopologues or it might be associated with changes in the excited state dynamics due to the impact of the isotope exchange on the strength of the hydrogen bonding network in the ASW. Either effect may possibly impact on the propagation of excitons to the vacuum interface and the resultant EIC.

At the most fundamental level, the mechanism of H_2 formation proposed by Kimmel and co-workers is probably the same as that of the fast C_6H_6 desorption from ASW. The key difference is that the electronically excited H_2O molecule at the C_6H_6 interface transfers the excitation to the hydrogen-bonded aromatic ring allowing this to desorb (Reactions (vi_a) and (vi_b)), rather than leading to H_2O desorption or bond cleavage:

$$H_2O^* + C_6H_6 \rightarrow H_2O + C_6H_6^* \hspace{4cm} (x)$$

$$C_6H_6^* \rightarrow C_6H_6(g) \hspace{5cm} (xi)$$

In fact, EPD of C_6H_6 from solid H_2O surfaces involves rather complex kinetics, which can be phenomenologically reproduced by a multi-exponential decay and involves additional processes such as non-thermal diffusion of the aromatic molecule from the edges of C_6H_6 islands to dangling OH groups at the ASW interface and changes in the morphology of the H_2O/vacuum interface. However, for low C_6H_6 doses ($\leq$10 L) the fast component of the EPD traces is accurately described by Reactions (x) and (xi), that run in parallel with Reaction (vi_a) and hence can be compared to H_2 desorption. In previous work, we measured the cross-section for the fast non-thermal desorption of C_6H_6 from H_2O to be $(1.0\pm0.4) \times 10^{-15}$ cm^2 during irradiation with 250 eV electrons.[21,32] In order to quantitatively compare the cross-sections corresponding to Reactions (vi), (x) and (xi), it is necessary to estimate the kinetics of H_2 desorption. Therefore, the EIC curves for H_2 and D_2 in Figure 2 have been normalized with respect to each maximum and have been plotted in Figure 3 along with a fitting function.
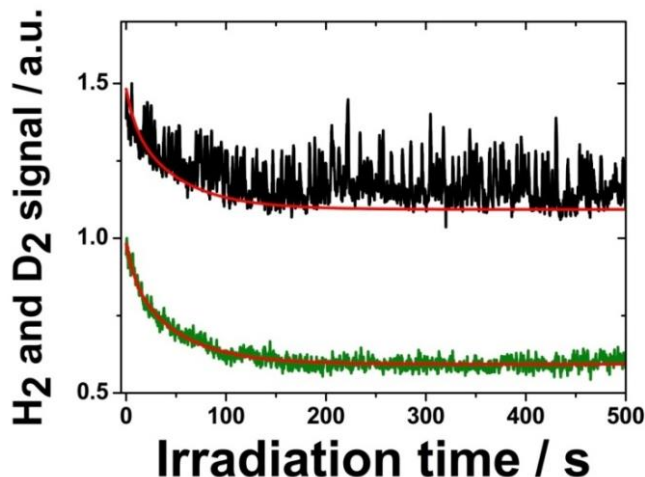
Figure 3. H_2 and D_2 evolution during 250 eV electron irradiation of 1 L of C_6H_6 on a thick ice (150 L) of solid H_2O and on solid D_2O reported in black and in green, respectively. Traces have been offset for clarity and each curve has been normalized with respect to its highest value for ease of comparison. The red line represents a bi-exponential fit.

Given the quality of the m/z = 2 data, a good exponential fit while possible is challenging due to the signal-to-noise considerations. Conversely, D_2 desorption displays a good S/N and the data were fitted up to 500 s with the following expression:

$$I(t) = I_1 e^{-\sigma_1 \varphi t} + I_2 e^{-\sigma_2 \varphi t} + I_\infty \qquad (4)$$

where φ is the electron flux (in this case there was no need to scale it due to rastering), σ_1 and σ_2 are the cross-sections in cm^2 for the two components of the decay, I_1 and I_2 are the corresponding amplitudes, while I_∞ is the residual. The same fitting function as derived from the D_2 kinetics is superimposed on both EIC traces in Figure 3. The agreement with the experimental data is rather good for D_2. While this is less convincing for H_2, the fit does provide a sensible representation of the overall H_2 appearance kinetics from solid H_2O, especially in the first 50 s where the fast component is most relevant.

	C_6H_6/H_2O	C_6H_6/H_2O
	$EIC(H_2)$	$EPD(C_6H_6)$
σ_1 / cm^2	$(1.0\pm0.2) \times 10^{-15}$	$(1.0\pm0.4) \times 10^{-15}$
σ_2 / cm^2	$(2.7\pm0.5) \times 10^{-16}$	$(6\pm2) \times 10^{-17}$

Table 2: List of values for the cross-sections corresponding to the fast and slow components observed in the EPD study of 5 L C_6H_6 from ASW and the EIC study of H_2 desorption from 250 eV electron irradiated ASW capped with 1 L of C_6H_6. The EPD values shown for C_6H_6/H_2O area also found in references 21 and 32 where further details can be found.

The values for the cross-sections are reported in Table 2 along with the analogous values obtained for EPD of C_6H_6 from ASW surfaces. It is noticeable that by analyzing the variation of the desorption signal, whether of H_2 or C_6H_6, some common kinetic features are found for both cases. Firstly, the recorded traces show a similar immediate rise when the irradiation begins, followed by a bi-exponential decay comprised of a fast and a slow component. Secondly and most importantly, the cross-section corresponding to the fast event is the same within the error bars providing semi-quantitative evidence for the assumed common initial mechanism in these two distinct processes. It follows that the energy transfer from the excited H_2O to the aromatic ring followed by C_6H_6 desorption (Reactions (x) and (xi)) or the dissociation of H_2O to subsequently form H_2 occur in parallel at the interface of the solid H_2O. Observing these species in a parallel kinetics fashion leads to the observation of a single common cross-section reflecting the sum of the cross-sections for the individual parallel processes. Without additional measurements of the relative yields (branching ratio) of the parallel channels, we cannot

definitively give individual cross-sections for the two processes. In contrast, the slow component is longer for EIC with respect to C_6H_6 EPD implying that additional steps should be taken into account in order to explain the decay at longer times.

It is important to stress that the observed traces are the result of several processes that take place as competitive and parallel kinetics during the electron irradiation. The mechanism so far presented does not explain the reason why an exponential decay, as per Equation 2, is observed. However, assuming a partially common mechanism for both C_6H_6 (EPD) and H_2 (EIC) desorption from ASW, some similarity between the kinetics of the two systems should be expected. This is supported by our data. In contrast, at longer times, other processes such as surface roughening and erosion, diffusion, and the formation of reactive species (H_2O_2, HO_2), will introduce additional differences between the EPD of C_6H_6 and the EIC followed by desorption of H_2. Indeed, there is still noticeable agreement between slow H_2 production (see Table 2) and overall H_2O loss reported in Table 1. In conclusion, although the RAIRS experiment cannot probe fast processes on and in the ASW, it does provide an important window on long timescale processes associated with electron irradiation given that by controlling the electron flux we can control the timescale of the processing.

Looking at H_2O desorption in Figure 2, the data are ambiguous to say the least. However, there does appear to be a small initial H_2O signal that tracks the H_2 trace. This could point to direct desorption of H_2O at the vacuum interface termini of the hydrogen bond networks responsible for exciton transport due directly to exciton relaxation. Equally, this low desorption signal could point to energy transfer from the terminal H_2O in such networks to adsorbed C_6H_6 at the ASW surface favoring reactions (x) and (xi) instead. As we have previously demonstrated, direct photo-excitation of C_6H_6 on H_2O in the near-UV around 250 nm (4.96 eV) is extremely efficient

in producing H_2O in the gas phase *via* an indirect adsorbate-mediated channel.[23,24,38] Energy transfer from the 8-12 eV exciton in ASW and subsequent non-radiative relaxation (internal conversion) of the electronically excited C_6H_6 would reflect this adsorbate-mediated channel and could provide for an efficient indirect desorption mechanism for the interfacial H_2O and for adsorbates like C_6H_6. Further experiments are clearly needed to explore which mechanism is at play in producing the small, observed H_2O signal.

4. Astrophysical Implications and Conclusions

In concluding this paper, let us first state that the reported EPD cross-section for H_2O reported in reference 38 is incorrect as the e^- beam raster correction was incorrectly applied. Given that, these present observations do not impact on our previously reported conclusions;

- Loss of water from ASW films is promoted by interaction with low-energy electrons.[38]

- The cross-section for the loss process is significantly larger than that for photon-promoted desorption and so electron-promoted desorption is likely to be the dominant desorption channel in cold, dense environments.[38]

As we reported in that work, a simple model based on conditions found in the object Barnard 68 over–estimated the cold core gas phase H_2O concentration by a significant factor. However, our observation herein of a weak H_2O desorption signal may explain this discrepancy and hence, to some degree, the observed gas-phase H_2O abundance in cold, dense environments.[49]

This now brings us to our present observations and the conclusions we can draw in relation to them;

- H_2 and O_2 are probably the dominant gas phase products from electron irradiation of ASW under the present conditions at a temperature of 100 K. The kinetics of the D_2

appearance measured by QMS beyond *ca.* 20 s in Figure 3, are essentially identical to those of the H_2O loss probed by RAIRS in Figure 1 when appropriate electron flux corrections are applied (non-rastered versus rastered). Understanding the composition of the desorbing material, *i.e.* the branching ratio into various product channels (both neutral and charged), is crucial to understanding the subsequent perturbation of the gas-phase chemistry by the species desorbing during electron irradiation of ASW. It is also important to understand this as a function of temperature as lowering of the grain temperature will slow diffusion and likely result in retention of less volatile products *e.g.* O_2.

- Intact H_2O is not the major desorption product observed, rather the molecular fragments of H_2 and O_2 are.

- The low H_2O yield might help correct the over-estimation of gas phase H_2O in our previous model.[38,50]

Table 2 highlights intriguing common kinetic features between EIC in ASW and EPD of hydrogen bonded molecules at the ASW surface under the present experimental conditions. These findings lead one to question the interplay between EIC and EPD for other ices, such as those containing methanol (CH_3OH), and how this relates to the desorption of COMs in cold environments. In fact, there is evidence for the observation of COMs in cold dense environments, see for instance the review by Tielens and references therein.[1] Both photon- and charged particle-induced desorption have been proposed as mechanisms to promote this. However, where the photons are ionizing, the basic physical processes occurring in ASW are identical to those expected for electron- and ion-irradiation and will yield neutral and charged atoms and molecules derived from a complex solid state chemistry. Non-thermal whole molecule

desorption by these processes is likely a very minor channel especially in reduced dimensional hydrogen bond network and organic-rich solids.[51] This would point to alternative desorption mechanisms for COM evolution into the gas phase. At present, desorption promoted by reaction enthalpy release is suggested.[52,53] An alternative scenario involving ice film disruption in grain-grain collisions has also been proposed. Further experimental work is necessary to identify which is the likely mechanism.

AUTHOR INFORMATION

Corresponding Author

*Contact information: ar163@hw.ac.uk or m.r.s.mccoustra@hw.ac.uk

Present Addresses

†Science Division, Jet Propulsion Laboratory, California Institute of Technology, Pasadena, CA 91109, USA

‡Physikalisches Institut, Westfälische Wilhelms-Universität Münster, Münster, Germany

Author Contributions

The manuscript was written through contributions of all authors. All authors have given approval to the final version of the manuscript.

REFERENCES

(1) Tielens, A. G. G. M., The Molecular Universe, *Rev. Mod. Phys.*, **2013**, *85*, 1021-1081.

(2) Bergin, E. A.; Maret, S.; Van der Tak, F. F. S.; Alves, J.; Carmody, S. M.; Lada, C. J., The Thermal Structure of Gas in Prestellar Cores; A Case Study of Barnard 68, *Astrophys. J.,* **2006**, *645*, 369-380.

(3) Cuppen, H. M.; Herbst, E., Simulation of the Formation and Morphology of Ice Mantles on Interstellar Grains, *Astrophys. J.*, **2007**, *668*, 294-309.

(4) Ioppolo, S.; Cuppen, H. M.; Romanzin, C.; van Dishoeck, E. F.; Linnartz, H., Water Formation at Low Temperature by Surface O_2 Hydrogenation I: Characterization of Ice Penetration, *Phys. Chem. Chem. Phys.*, **2010**, *12*, 12065-12076.

(5) Cuppen, H. M.; Ioppolo, S.; Romanzin, C.; Linnartz, H., Water Formation at Low Temperature by Surface O_2 Hydrogenations II: The Reaction Network, *Phys. Chem. Chem. Phys.*, **2010**, *12*, 12077-12088.

(6) Mokrane, H.; Chaabouni, H.; Accolla, M.; Congiu, E.; Dulieu, F.; Chehrouri, M.; Lemaire, J. L., Experimental Evidence for Water Formation Via Ozone Hydrogenation on Dust Grains at 10 K, *Astrophys. J. Lett.*, **2009**, *705*, L195.

(7) Taylor, S.; Williams, D., Star Studded Chemistry, *Chemistry in Britain*, **1993**, 680-683.

(8) Capria, M. T., Sublimation Mechanism of Comet Nuclei, *Earth Moon Planets*, **2000**, *89*, 161-178.

(9) May, R. A.; Smith, R. S.; Kay, B. D., The Release of Trapped Gases from Amorphous Solid Water films. I. "Top-Down" Crystallization-Induced Crack Propagation Probed using the Molecular Volcano, *J. Chem. Phys.*, **2013**, *138*, 104501.

(10) Cazaux, S.; Tielens, A. G. G. M.; Ceccarelli, C.; Castets, A.; Wakelam, V.; Caux, E.; Parise, B.; Teyssier, D., The Hot Core around the Low-Mass Protostar IRAS 16393-2422: Scoundrels Rule! *Astrophys. J*, **2003**, *593*, L51.

(11) Martín-Doménech, R.; Muñoz Caro, G. M.; Bueno, J.; Goesmann, F., Thermal Desorption of Circumstellar and Cometary Ice Analogs, *Astron Astrophys*, **2014**, *564*, A8.

(12) Jones, P.; Williams, D. A., The 3 μm Ice Band in Taurus: Implications for Interstellar Chemistry, *Mon. Not. R. Astron. Soc*, **1984**, *209*, 955-960.

(13) Schutte, W. A.; Allamandola, L. J.; Sandford, S A., An Experimental Study of the Organic Molecules Produced in Cometary and Interstellar Ice Analogs by Thermal Formaldehyde Reactions, *Icarus*, **1993**, *104*,118-137.

(14) Collings, M. P.; Dever, J. W.; Fraser, H. J.; McCoustra, M. R. S., Laboratory Studies of the Interaction of Carbon Monoxide with Water Ice, *Astrophys. Space. Sci.*, **2003**, *285*, 633-659.

(15) Collings, M. P.; Anderson, M. A.; Chen, R.; Dever, J. W.; Viti, S.; Williams, D. A.; McCoustra, M. R. S., A Laboratory Survey of the Thermal Desorption of Astrophysically Relevant Molecules, *Mon. Not. R. Astron. Soc.*, **2004**, *354*, 1133-1140.

(16) Theulé, P.; Duvernay, F.; Danger, G.; Borget, F.; Bossa, J. B.; Vinogradoff, V.; Mispelaer, F.; Chiavassa, T., Thermal Reactions in Interstellar Ice: A Step Towards Molecular Complexity in the Interstellar Medium, *Adv. Space Res*., **2013**, *52*, 1567-1579.

(17) Lippok, N.; Launhardt, R.; Semenov, D.; Stutz, A. M.; Balog, Z.; Henning, Th.; Krause, O.; Linz, H.; Nielbock, M.; Pavlyuchenkov, Ya. N.; Schmalzl, M.; Schmiedeke, A.; Bieging, J. H., Gas-Phase CO Depletion and N_2H^+ Abundances in Starless Cores, *Astron Astrophys*, **2013**, *560*, A41.

(18) Fayolle, E. C.; Bertin, M.; Romanzin, C.; Michaut, X.; Oberg, K. I.; Linnartz, H.; Fillion, J.–H., CO Ice Photodesorption: A Wavelength-dependent Study, *Astrophys. J. Lett*, **2011**, *739*, L36.

(19) Keto, E.; Rawlings, J.; Caselli, P., Chemistry and Radiative Transfer of Water in Cold, Dense Clouds, *Mon. Not. R. Astron. Soc.*, **2014**, *440*, 2616-2624.

(20) Dartois, E.; Auge, B.; Boduch, P.; Brunetto, R.; Chabot, M.; Domaracka, A.; Ding, J. J.; Kamalou, O.; Lv, X. Y.; Rothard, H.; da Silveira, E. F.; Thomas, J. C., Heavy Ion Irradiation of Crystalline Water Ice: Cosmic Ray Amorphisation Cross-Section and Sputtering Yield, Astron. Astrophys., **2015**, *576*, A125.

(21) Marchione, D.; Thrower, J. D.; McCoustra, M. R. S., Efficient Electron-Promoted Desorption of Benzene from Water Ice, *Phys. Chem. Chem. Phys.*, **2016**, *18*, 4026-4034.

(22) Marchione, D.; McCoustra, M. R. S., Electrons, Excitons and Hydrogen Bonding: Electron-Promoted Desorption from Molecular Ice Surfaces, *Phys. Chem. Chem. Phys.*, **2016**, *18*, 29747-29755.

(23) Thrower, J. D.; Collings, M. P.; McCoustra, M. R. S.; Burke, D. J.; Brown, W. A.; Dawes, A.; Holtom, P. D.; Kendall, P.; Mason, N. J.; Jamme, F.; Fraser, H. J.; Clark, I. P.; Parker, A. W., Surface Science Investigations of Photoprocesses in Model Interstellar Ices, *J. Vac. Sci. Technol. A*, **2008**, *26*, 919-924.

(24) Thrower, J. D., Laboratory Investigations of the Thermal and Non-Thermal Processing of Condensed Aromatic Hydrocarbons in the Interstellar Medium, *Ph.D. Thesis*, Heriot-Watt University, Edinburgh, 2009.

(25) Fraser, H. J.; Collings, M. P.; McCoustra, M. R. S.; Williams, D. A., Thermal Desorption of Water Ice in the Interstellar Medium, *Mon. Not. R. Astron. Soc*, **2001**, *327*, 1165-1172.

(26) Collings, M. P.; Frankland, V. L.; Lasne, J.; Marchione, D.; Rosu-Finsen, A.; McCoustra, M. R. S., Probing Model Interstellar Grain Surfaces with Small Molecules, *Mon. Not. R. Astron. Soc.*, 2015, 449, 1826-1833.

(27) Rosu-Finsen, A.; Marchione, D.; Salter, T. L.; Stubbing, J. W.; Brown, W. A.; McCoustra, M. R. S., Peeling the Astronomical Onion, *Phys. Chem. Chem. Phys.*, **2016**, *18*, 31930-31935.

(28) Sieger, M. T.; Orlando, T. M., Probing Low-Temperature Water Ice Phases Using Electron-Stimulated Desorption, *Surf. Sci.*, **2000**, *451*, 97-101.

(29) Zheng, W.; Jewitt, D.; Kaiser, R. I., Formation of Hydrogen, Oxygen, and Hydrogen Peroxide in Electron-Irradiated Crystalline Water Ice, *Astrophys. J.*, **2006**, *639*, 534-548.

(30) Toennies, J. P.; Traeger, F.; Vogt, J.; Weiss, H., Low-Energy Electron Induced Restructuring of Water Monolayers on NaCl(100), *J. Chem. Phys.*, **2004**, *120*, 11347-11350.

(31) Grieves, G. A.; Orlando, T. M., The Importance of Pores in the Electron Stimulated Production of D_2 and O_2 in Low Temperature Ice, *Surf. Sci.*, **2005**, *593*, 180-186.

(32) Thrower, J. D.; Collings, M. P.; Rutten, F. J. M.; McCoustra, M. R. S., Highly Efficient Electron-Stimulated Desorption of Benzene from Amorphous Solid Water Ice, *Chem. Phys. Lett.*, **2011**, *505*, 106-111.

(33) Oberg, K. I.; Linnartz, H.; Visser, R.; van Dishoeck, E. F.,Photodesorption of Ices. II. H_2O and D_2O, *Astrophys. J.*, **2009**, *693*, 1209-1218.

(34) Bertin, M.; Romanzin, C.; Doronin, M.; Philippe, L.; Jeseck, P.; Ligterink, N.; Linnartz, H.; Michaut, X.; Fillion, J.-H., UV Photodesorption of Methanol in Pure and CO-rich Ices: Desorption Rates of the Intact Molecule and of the Photofragments, *Astrophys. J. Lett.*, **2016**, *817*, L12.

(35) Abdulgalil, A. G. M.; Marchione, D.; Rosu-Finsen, A.; Collings, M. P.; McCoustra, M. R. S., Laboratory Investigations of Irradiated Acetonitrile-Containing Ices on an Interstellar Dust Analog, *J. Vac. Sci. Technol. A*, **2012**, *30*, 041505.

(36) Thrower, J. D.; Collings, M. P.; Rutten, F. J. M.; McCoustra, M. R. S., Laboratory Investigation of the Interaction Between Benzene and Bare Silicate Grains Surfaces, *Mon. Not. R. Astron. Soc.*, **2009**, *394*, 1510-1518.

(37) Summers, R. L., Empirical Observations on the Sensitivity of Hot Cathode Ionization Type Vacuum Gages, *NASA Technical Reports*, **1969**, NASA-TN-D-5285.

(38) Thrower, J. D.; Abdulgalil, A. G. M.; Collings, M. P.; McCoustra, M. R. S.; Burke, D. J.; Brown, W. A.; Dawes, A.; Holtom, P. J.; Kendall, P.; Mason, N. J.; Jamme, F.; Fraser, H. J.; Rutten, F. J. M., Photon- and Electron-Stimulated Desorption from Laboratory Models of Interstellar Ice Grains, *J. Vac. Sci. Technol. A*, **2010**, *28*, 799-806.

(39) Cottin, H.; Moore, M. H.; Bénilan, Y., Photodestruction of Relevant Interstellar Molecules in Ice Mixtures, *Astrophys. J.*, **2003**, *590*, 874-881.

(40) Gerakines, P. A.; Schutte, W. A.; Ehrenfreund, P., Ultraviolet Processing of Interstellar Ice Analogs. I. Pure Ices, *Astron. Astrophys*, **1996**, *312*, 289-305.

(41) Ehrenfreund, P.; Bernstein, M. P.; Dworkin, J. P.; Sandford, S. A.; Allamandola, L. J., The Photostability of Amino Acids in Space, *Astrophys. J.*, **2001**, *550*, L95.

(42) Andersson, S.; van Dishoeck, E. F., Photodesorption of Water Ice, *Astron. Astrophys.*, **2008**, *291*, 907-916.

(43) Petrik, N. G.; Kimmel, G. A., Electron-Stimulated Reactions at the Interface of Amorphous Solid Water Films Driven by Long-Range Energy Transfer from the Bulk, *Phys. Rev. Lett.*, **2003**, *90*, 166102.

(44) Petrik, N. G.; Kavetsky, A. G.; Kimmel, G. A., Electron-Stimulated Production of Molecular Oxygen in Amorphous Solid Water on Pt(111), *J. Chem. Phys.*, **2006**, *125*, 124702.

(45) Petrik, N. G.; Kavetsky, A. G.; Kimmel, G. A., Electron-Stimulated Production of Molecular Oxygen in Amorphous Solid Water, *J. Phys. Chem. B*, **2006**, *110*, 2723-2731.

(46) Petrik, N. G.; Kimmel, G. A., Electron-Stimulated Production of Molecular Hydrogen at the Interfaces of Amorphous Solid Water Films on Pt(111), *J. Chem. Phys.*, **2004**, *121*, 3736-3744.

(47) Petrik, N. G.; Kimmel, G. A., Electron-Stimulated Sputtering of Thin Amorphous Solid Water Films on Pt(111), *J. Chem. Phys.*, **2005**, *123*, 054702.

(48) Petrik N.G.; Kimmel, G. A., Electron-Simulated Reactions at the Interfaces of Amorphous Solid Water Films Driven by Long-Range Energy Transfer from the Bulk, *Phys. Rev. Lett.*, **2003**, *90*, 166102.

(49) van Dishoeck, E. F.; Helmich, F. P., Infrared Absorption of H_2O Toward Massive Young Stars, *Astron. Ap.*, **1996**, *315*, L177.

(50) Abdulgalil, A. G. M., Laboratory Surface and Solid State Astrochemistry of Bimolecular Precursors on Grain Mimics, *Ph.D. Thesis*, Heriot-Watt University, Edinburgh, 2013.

(51) Marchione, D.; McCoustra, M. R. S., Electrons, excitons and hydrogen bonding: electron-promoted desorption from molecular ice surfaces, *Phys. Chem. Chem. Phys.*, **2016**, 18, 29747-29755.

(52) Rawlings, J. M. C.; Williams, D. A.; Viti, S.; Cecchi-Pestellini, C.; Duley, W. W., Episodic Explosions in Interstellar Ices, *Mon. Not. R. Astron. Soc.*, **2013**, *430*, 264-273.

(53) Cecchi-Pestellini, C.; Rawlings, J. M. C.; Viti, S.; Williams, D. A., Chemistry in Evaporating Ices – Unexplored Territory, *Astrophys. J.*, **2010**, *725*, 1581-1586.

For TOC only: